Electronic Supplementary Material (ESI) for Journal of Materials Chemistry A.

Supporting Information

Efficient and durable vanadium flow battery enabled by high-performance fluorinated poly(aryl piperidinium) membranes

Tao Ban, Maolian Guo, Yajie Wang, Jiawang Ma, Xinxin Wang, Zihui Wang, and Xiuling Zhu*.

State Key Lab of Fine Chemicals, Department of Polymer Science & Materials,

Dalian University of Technology,

Dalian 116024, China

Table of Contents

1. Experimental section 1

1.1 Materials 1

1.2 Synthesis of fluorinated poly(triphenyl piperidine) (PFMP-x) 1

1.4 Preparation of anion exchange membranes 2

1.5 Synthesis of poly(isatin- methyl piperidine-terphenyl) (PIMP-90). 3

1.6 Quaternization of poly(isatin- methyl piperidine-terphenyl) (PIDP-90). 3

1.7 Membrane preparation. 3

2. Results and Discussion 4

References 24

1. Experimental section

1.1 Materials

Pentafluorobenzaldehyde (98%), N-methyl-4-piperidone (98%), indole-2,3-dione (isatin, 98%), p-terphenyl (98%), trifluoromethanesulfonic acid (99%), trifluoroacetic acid (99%), and iodomethane (99.5%) were purchased from Anhui Zesheng Technology Co. Ltd. Vanadyl sulfate ($VOSO_4$, 98 %) was provided by Shanghai Yuanfan Biotechnology Co. Ltd. Anhydrous magnesium sulfate ($MgSO_4$, 98 %) and anhydrous potassium carbonate (K_2CO_3, 98 %) were obtained from Tianjin Komiou Chemical Reagent Co. Ltd. Dichloromethane (DCM) and dimethyl sulfoxide (DMSO) were used after water removal.

1.2 Synthesis of fluorinated poly(triphenyl piperidine) (PFMP-x)

Copolymers of PFMP-x (where x denotes the molar percentage content of N-methyl-4-piperidone structural unit) in different proportions were prepared by the same method. A typical synthesis of PFMP-60 was performed as follows (the first step in Fig. S1): Pentafluorobenzaldehyde (10 mmol, 1.9610 g), N -methyl-4-piperidone (15 mmol, 1.6975 g) and p-terphenyl (20.833 mmol, 4.7981 g) were added to a 100 mL double-port glass reactor. Subsequently, 32 mL of CH_2Cl_2 was added to the reactor as the solvent and stirred with a mechanical stirrer. Then 3.2 mL of trifluoromethanesulfonic acid (dark green solution at this time) was slowly added and the reaction was carried out at room temperature for 8-12 h. The dark blue viscous reaction product was poured into 500 ml of deionized water and precipitated and cut into small pieces, and washed repeatedly with deionized water to neutral PH. Finally, it was dried under vacuum at 80 °C for 24 h to obtain white PFMP-60 with a yield of 92.5%.

1.3 Synthesis of fluorinated poly(triphenyl piperidinium) (PFDP-x)

For this preparation as shown in the second step of Fig. S1, PFMP-60 (5.0 g, 14 mmol) was completely dissolved in DMSO (100 mL) on a 250 mL single-necked flask with a magnetic stirrer. Subsequently, K_2CO_3 (3.8679 g, 28 mmol) and iodomethane (5.9615 g, 42 mmol) were added to the polymer solution and the reaction was carried out at 40 °C under completely light-proof conditions for 24 h. The polymer solution was precipitated in ethyl acetate, filtered, and washed several times with deionized water to remove the residual iodomethane and salt. The

flocculated polymer was dried in an oven at 80 ℃ for 24 h to obtain light yellow PFDP-60 in 89% yield.

1.4 Preparation of anion exchange membranes

Briefly, 2 g poly(triphenyl piperidinium) (PFDP-x) containing pentafluorophenyl was dissolved in 40 mL DMSO solution and prepared as 5 % of the cast membrane solution. After filtration, the solution was poured onto a clean glass plate, dried at 80 °C for 24 h, and then dried under vacuum at 100 °C for another 12 h to completely remove the solvent. Eventually, large-size membranes (40±5 μm) were obtained after being peeled off from the glass plates (Figure 1b).

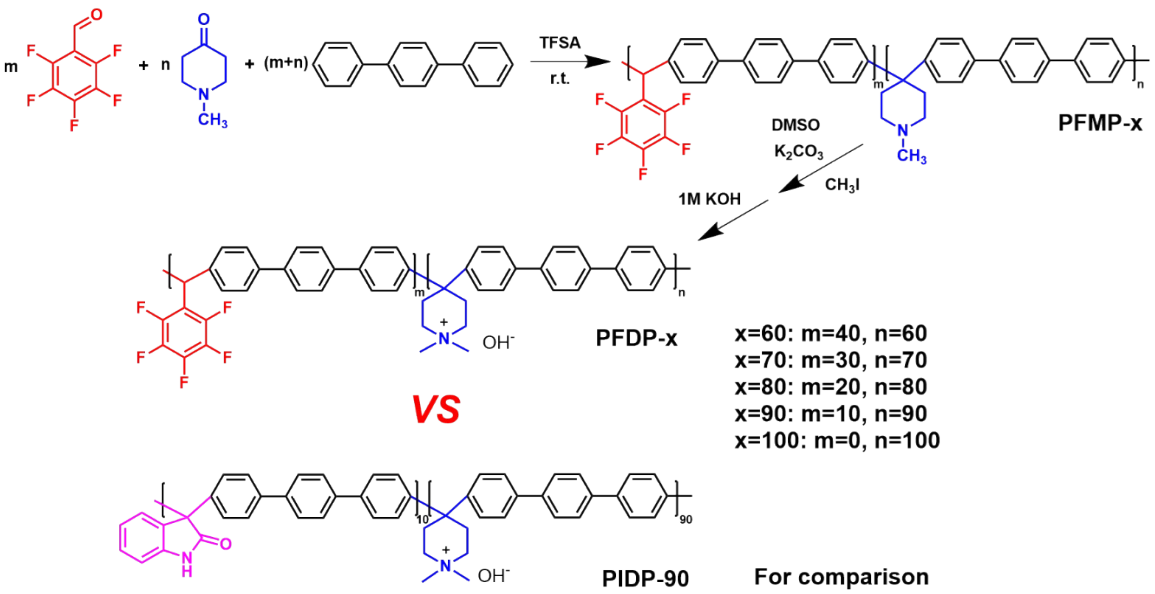

Fig. S1 Synthetic route of fluorinated poly(triphenyl piperidinium) (PFDP-x).

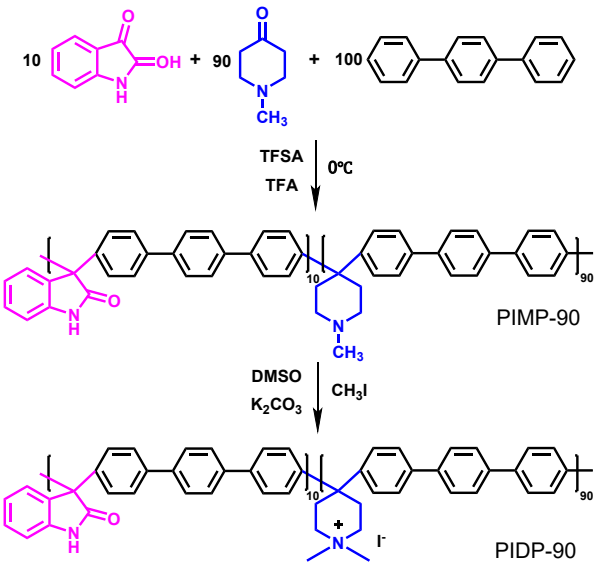

Fig. S2 Synthesis of polymer precursor PIMP-90 and ionic polymer PIDP-90.

1.5 Synthesis of poly(isatin- methyl piperidine-terphenyl) (PIMP-90).

Poly(isatin-methyl piperidine-terphenyl) (PIMP-90) copolymer was synthesized by superacid-catalyzed Friedel-Crafts alkylation reaction, where 90 is the feed ratio of piperidine in the total carbonyl compound. The specific steps were as follows (Fig. S2 first step): the monomer of isatin (0.7365 g, 5 mmol), N-methyl-4-piperidone (5.0921 g, 45 mmol), and p-terphenyl (10.4686 g, 45.5 mmol) was added to the double-mouth flask, and 8.73 mL of dichloromethane was added to the reactor with mechanical stirring. Subsequently, the trifluoromethanesulfonic acid (7.2 mL) and trifluoroacetic acid (0.74 mL) were slowly added to the reactor under an ice bath, and the reaction solution was dark green at this time, and the reaction was removed after 24 h in an ice water bath and washed repeatedly with deionized water and sodium bicarbonate until neutral. The reaction solution was dried under vacuum at 100°C for 24 h to obtain a yellow copolymer with a yield of 92.1%.

1.6 Quaternization of poly(isatin- methyl piperidine-terphenyl) (PIDP-90).

The quaternization reaction was performed as the second step in Fig. S2, and the quaternized polymer synthesized in this experiment was named PIDP-90. The specific steps were referred to as the synthesis of fluorinated poly(triphenyl piperidinium) (PFDP-x). A light-yellow PIDP-90 flocculent product was finally obtained at a yield of 88%.

1.7 Membrane preparation.

The preparation process of PIDP-90 AEM was the same as the anion exchange membranes preparation process in part 1.4 above.

2. Results and Discussion

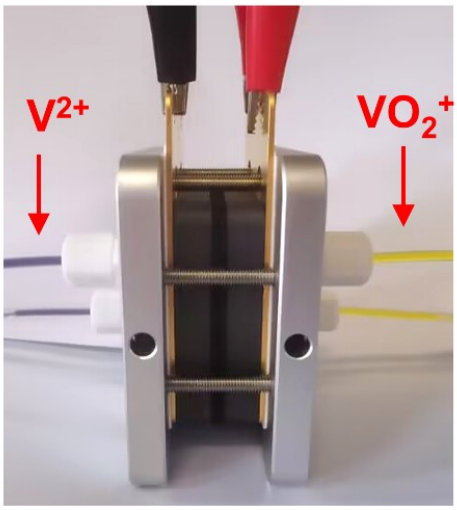

Fig. S3 Photograph of a vanadium flow battery in the fully charged state. The cathode electrolyte is orange VO_2^+ and the anode electrolyte is purple V^{2+}.

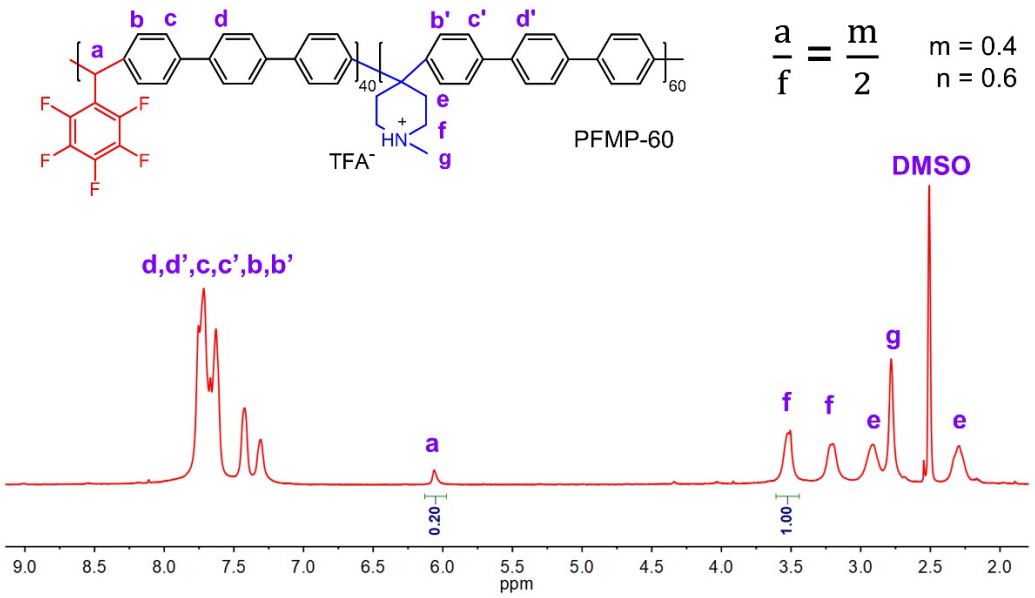

Fig. S4 ^{1}H-NMR spectrum of PFMP-60. DMSO-d_6 was utilized as the NMR solvent and 5 vol% TFA was employed as a co-solvent to remove the effect of H_2O.

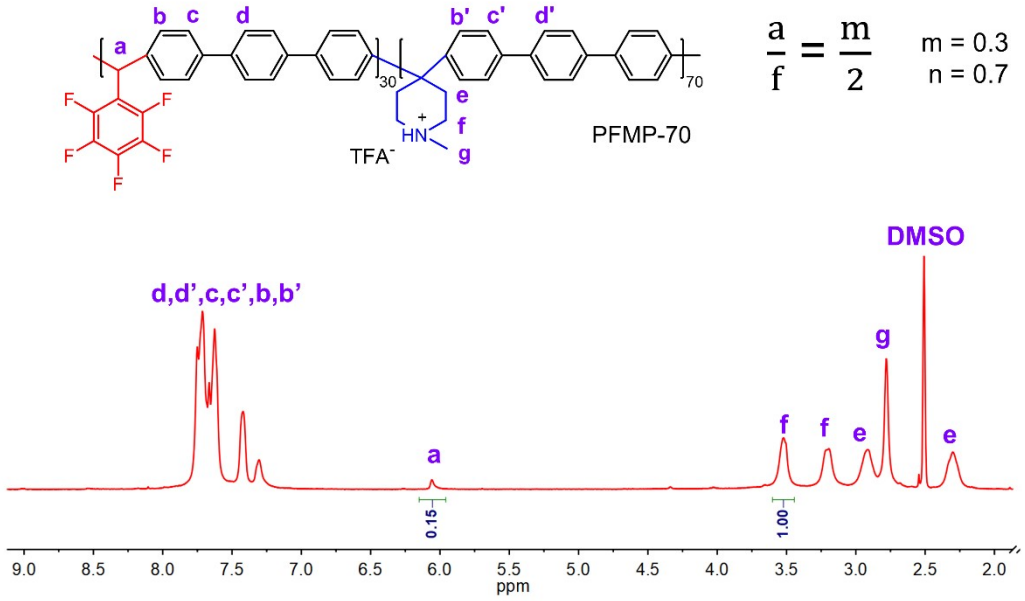

Fig. S5 ^{1}H-NMR spectrum of PFMP-70. DMSO-d_6 was utilized as the NMR solvent and 5 vol% TFA was employed as a co-solvent to remove the effect of H_2O.

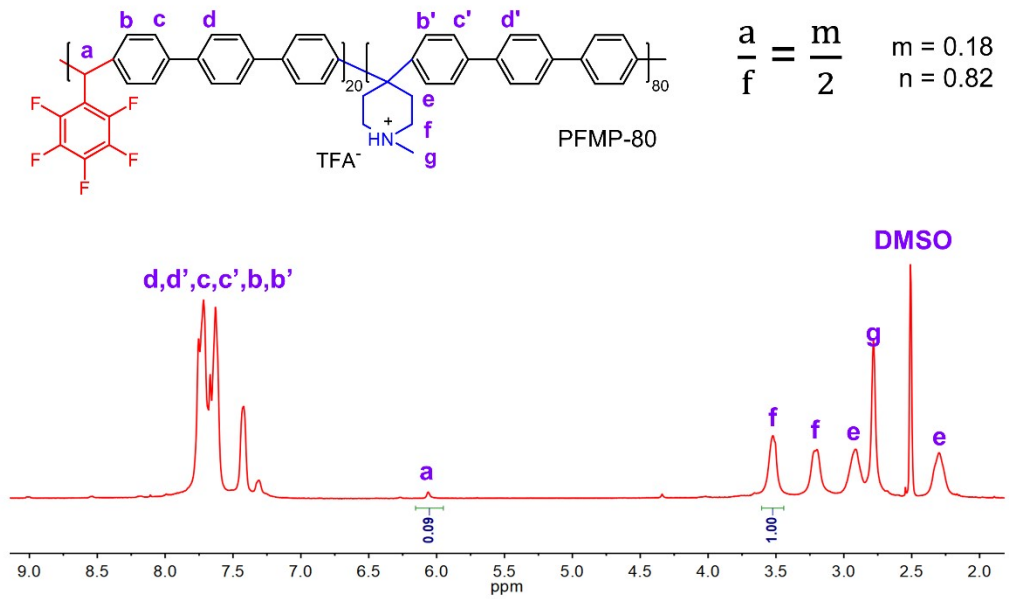

Fig. S6 ^{1}H-NMR spectrum of PFMP-80. DMSO-d_6 was utilized as the NMR solvent and 5 vol% TFA was employed as a co-solvent to remove the effect of H_2O.

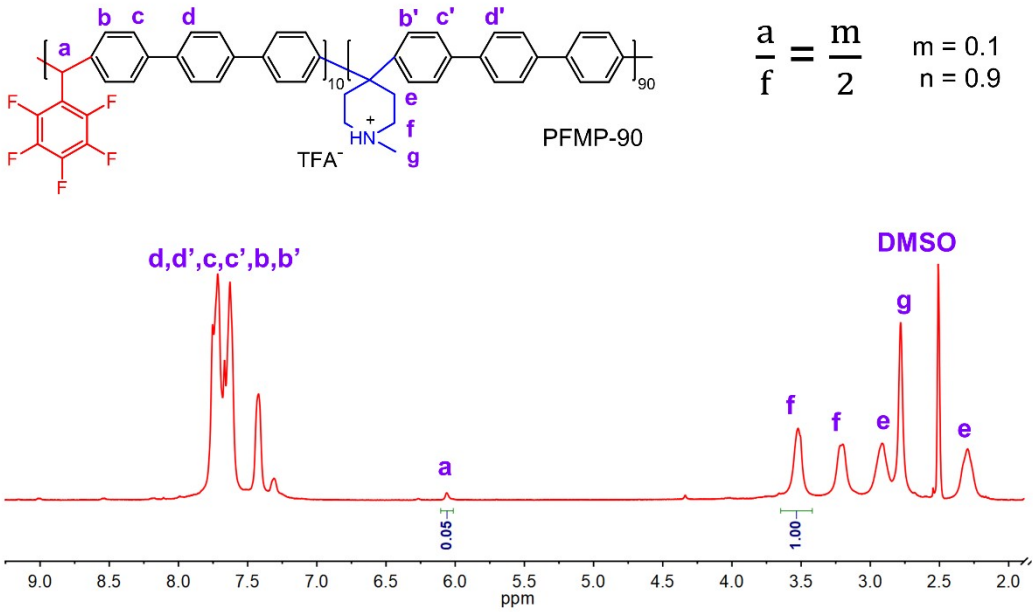

Fig. S7 ^{1}H-NMR spectrum of PFMP-90. DMSO-d_6 was utilized as the NMR solvent and 5 vol% TFA was employed as a co-solvent to remove the effect of H_2O.

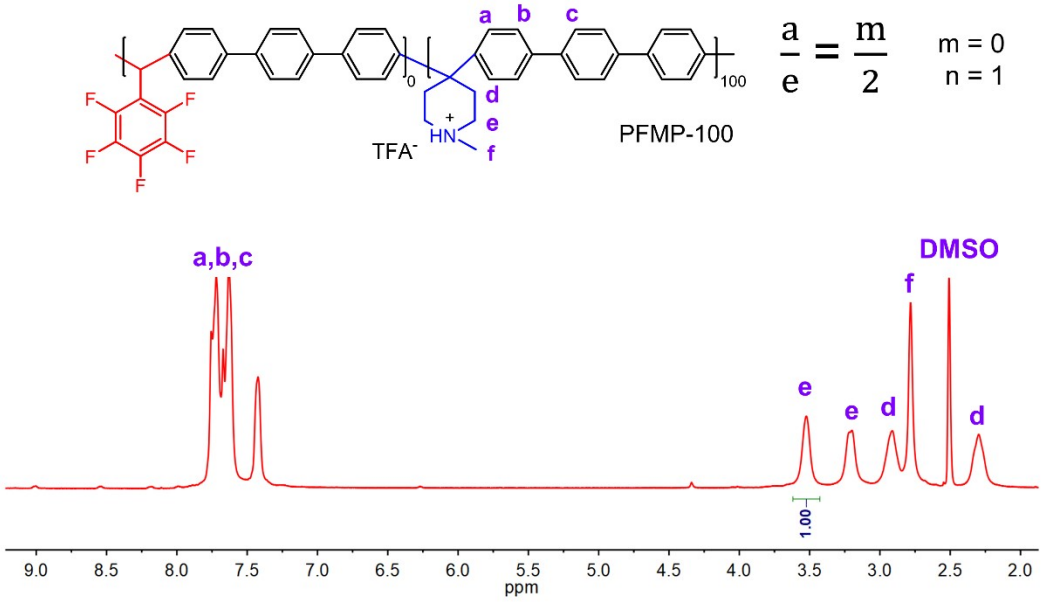

Fig. S8 ^{1}H-NMR spectrum of PFMP-100. DMSO-d_6 was utilized as the NMR solvent and 5 vol% TFA was employed as a co-solvent to remove the effect of H_2O.

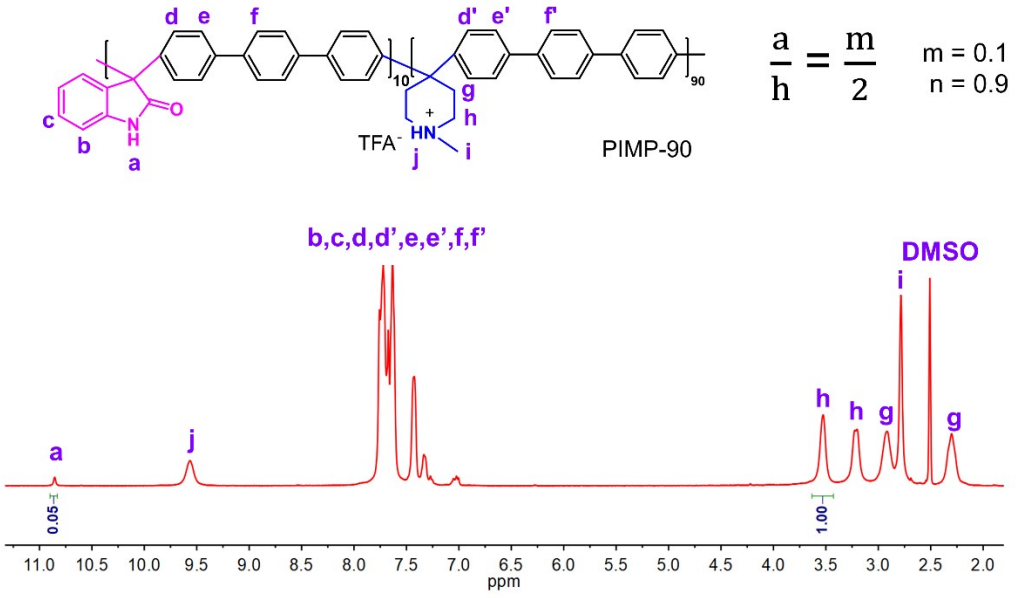

Fig. S9 ^{1}H-NMR spectrum of PIMP-90. DMSO-d_6 was utilized as the NMR solvent and 5 vol% TFA was employed as a co-solvent to remove the effect of H_2O.

Table S1. Percentage of fluorinated units, intrinsic viscosity (η), quaternization conditions and yield of PFDP-x[a] and PIDP-90 AEMs.

AEMs	Percentage of fluorinated units (%)	η (dL g^{-1})	Quaternization conditions	Yield (%)
PFDP-60	40	4.29	40℃ + 48 h	91.7
PFDP-70	30	4.12	40℃ + 48 h	90.3
PFDP-80	18	4.66	40℃ + 48 h	92.5
PFDP-90	10	4.07	40℃ + 48 h	94.1
PFDP-100	0	4.81	40℃ + 48 h	94.5
PIDP-90	0	4.76	40℃ + 48 h	91.9

[a] X is a molar ratio (percentage) of N-methyl-4 piperidone to aryl monomers.

Table S2. Solubility of different polymers in common solvents.

Polymers	DMF	DMAc	NMP	DMSO	Methanol	Isopropanol
PFDP-60	++	++	++	++	-	-
PFDP-70	++	++	++	++	-	-
PFDP-80	++	++	++	++	-	-
PFDP-90	++	++	++	++	-	-
PFDP-100	++	++	++	++	-	-
PIDP-90	++	++	++	++	-	-

++: dissolves well; -: did not dissolve.

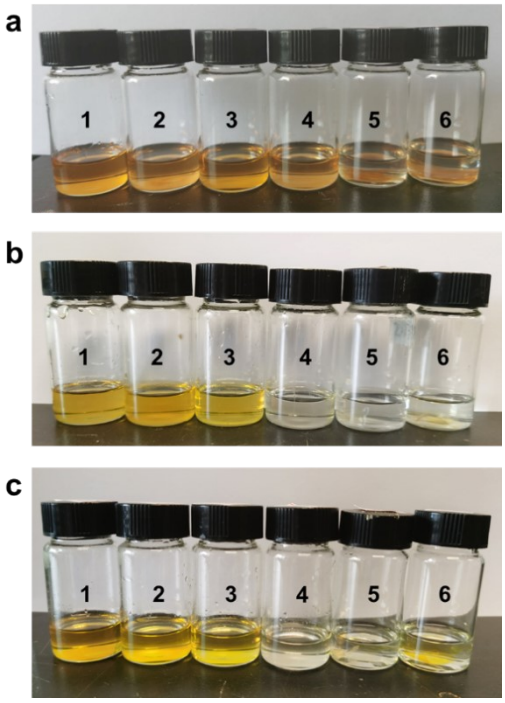

Fig. S10 Pictures of the solubility of a) PFDP-90, b) PFDP-100, c) PIDP-90 in various solvents (the solvent corresponding to the number, 1: DMF, 2: DMAc, 3: NMP, 4: DMSO, 5: Methanol, 6: Isopropanol).

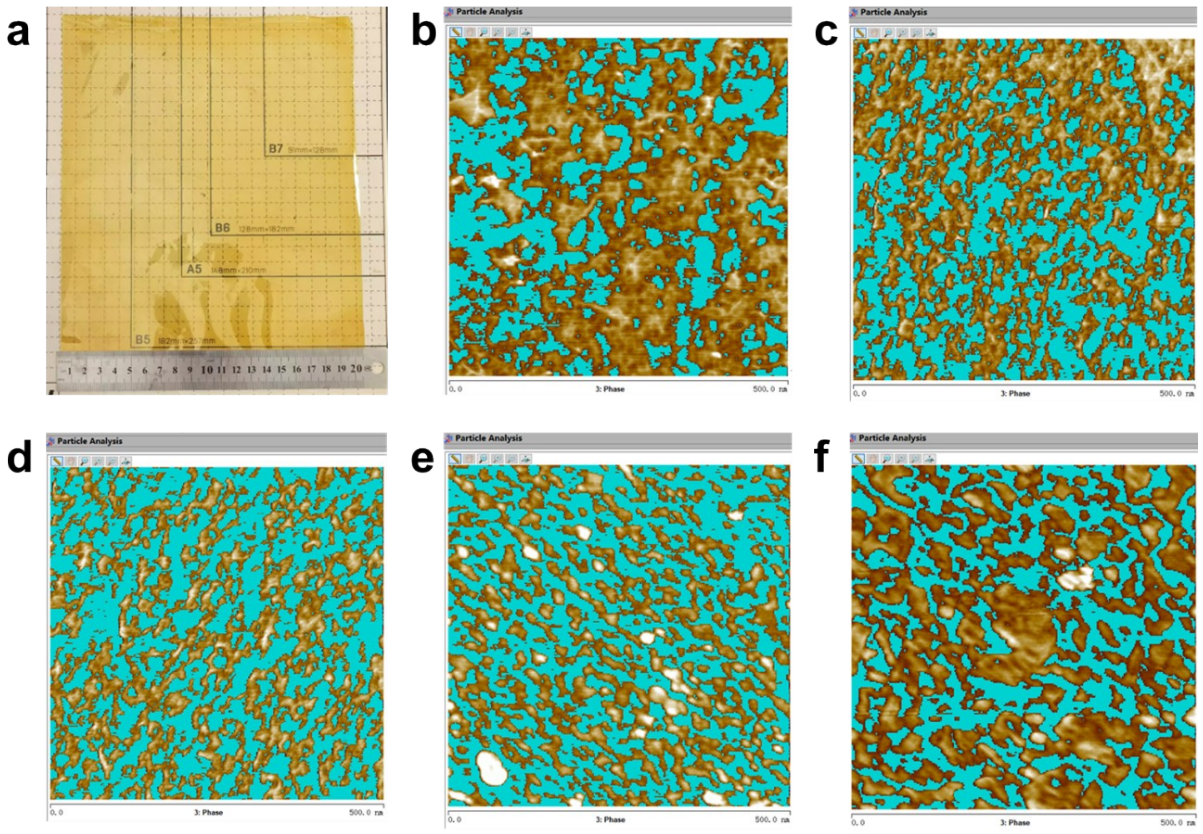

Fig. S11 a) Photographs of PFDP-90 membrane in 20×24 cm. Particle analysis of AFM phase diagram: b) PFDP-60, c) PFDP-70, d) PFDP-80, e) PFDP-90, f) PFDP-100.

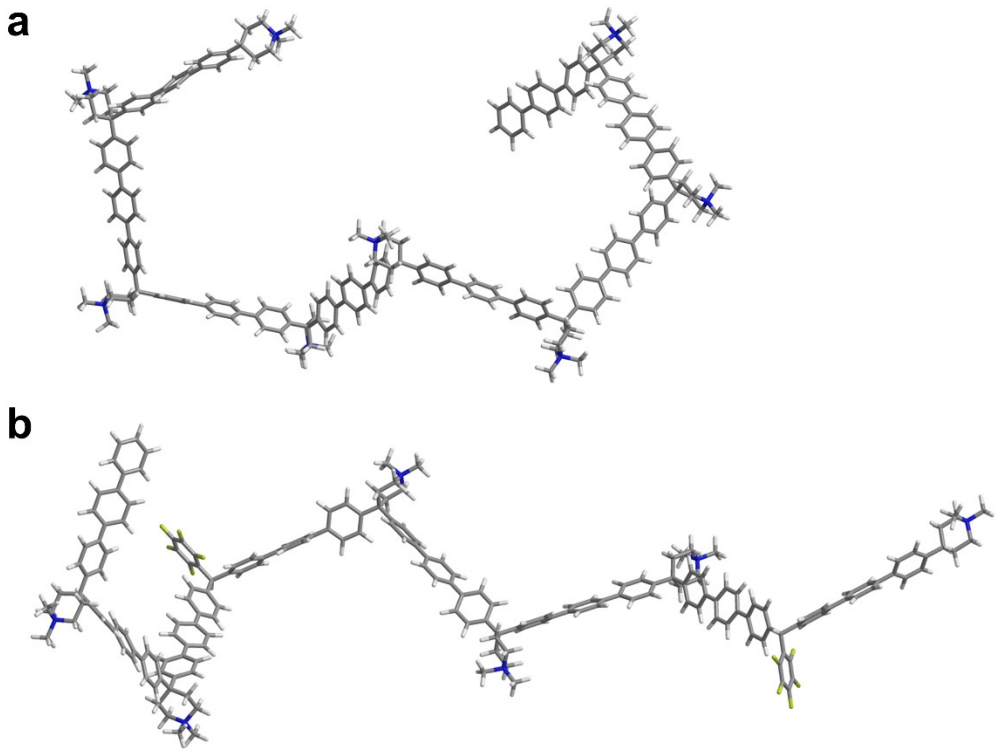

Fig. S12 Three-dimensional model structures of ionic polymers. (a) PFDP-100 (without fluorine structural unit), (b) PFDP-90 (with the fluorine-containing structural unit). Color codes: white for hydrogen, gray for carbon, blue for nitrogen, and sulfur for fluorine.

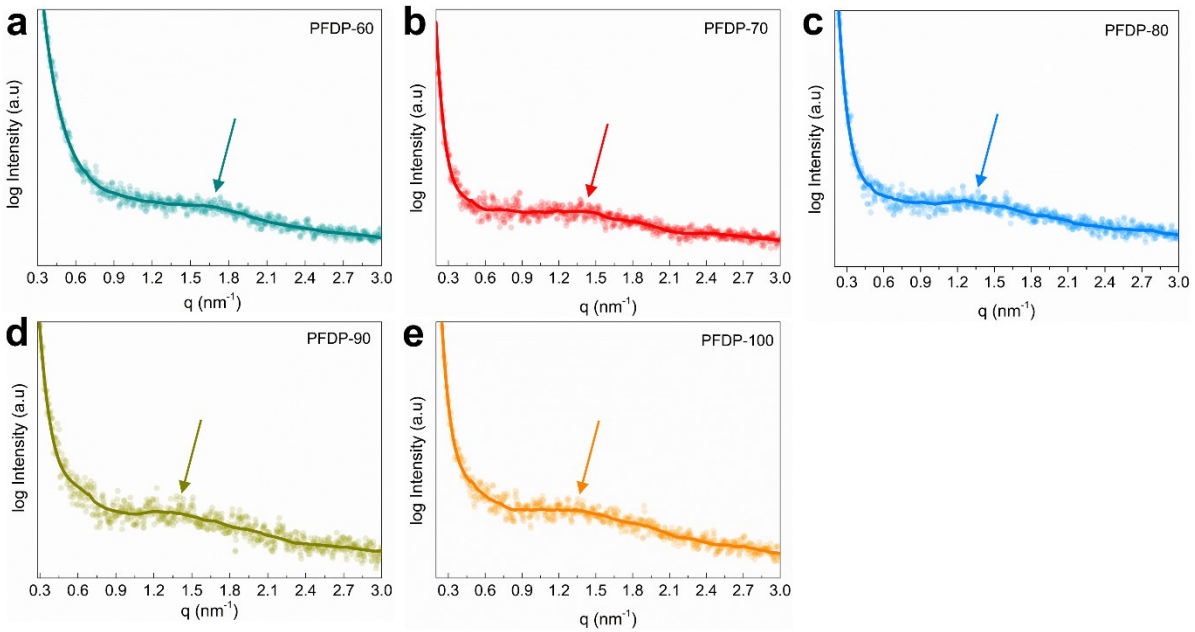

Fig. S13 a-e) SAXS profiles of dry PFDP-x AEMs in the I^- form.

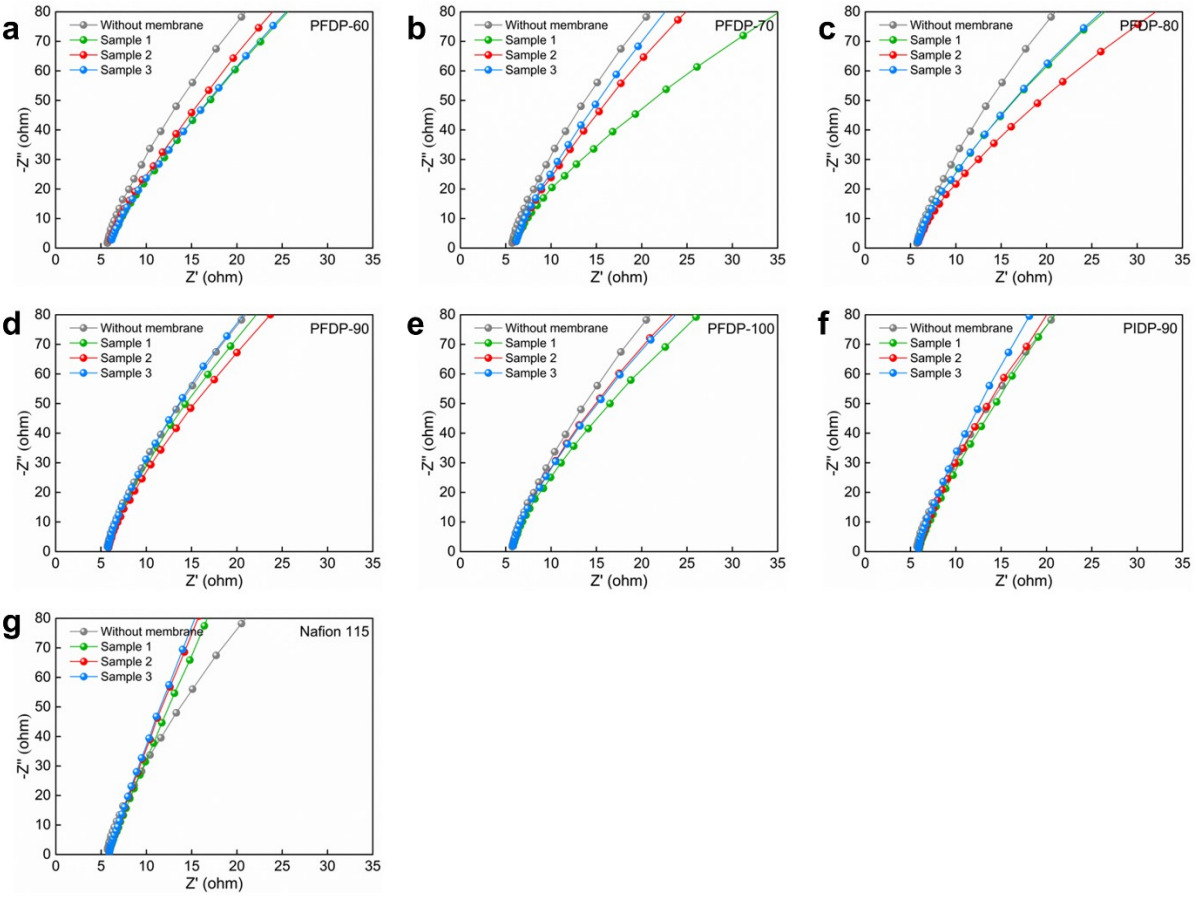

Fig. S14 a-g) Nyquist plots of PFDP, PIDP and Nafion 115 membranes in 3 M H_2SO_4 solution at room temperature were determined using EIS.

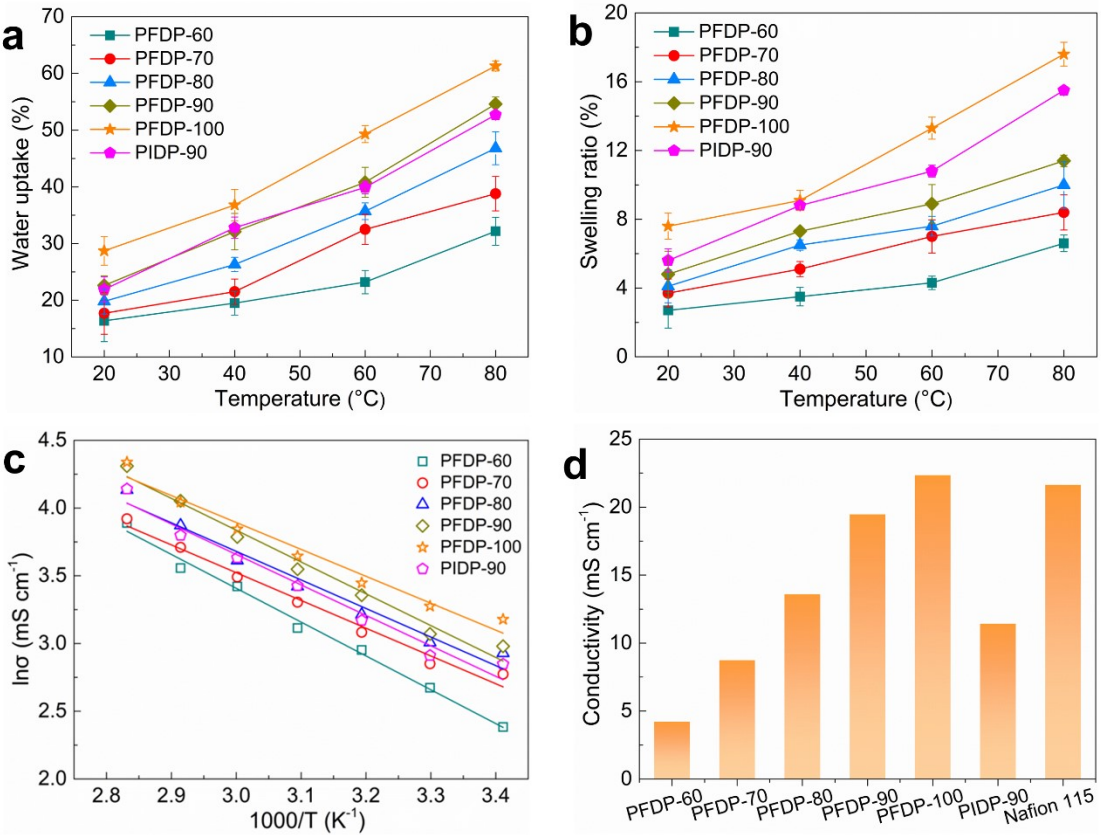

Fig. S15 a) Water uptake and b) swelling ratio of PFDP and PIDP membranes in deionized water at different temperatures. Error bars are based on standard deviations derived from three measurements of three different samples. c) Temperature dependence of ionic conductivity in the range of 20-80 ℃ for PFDP, PIDP and Nafion 115 membranes measured in deionized water. d) The ionic conductivity of PFDP, PIDP and Nafion 115 membranes under 3 M H_2SO_4 solution at room temperature.

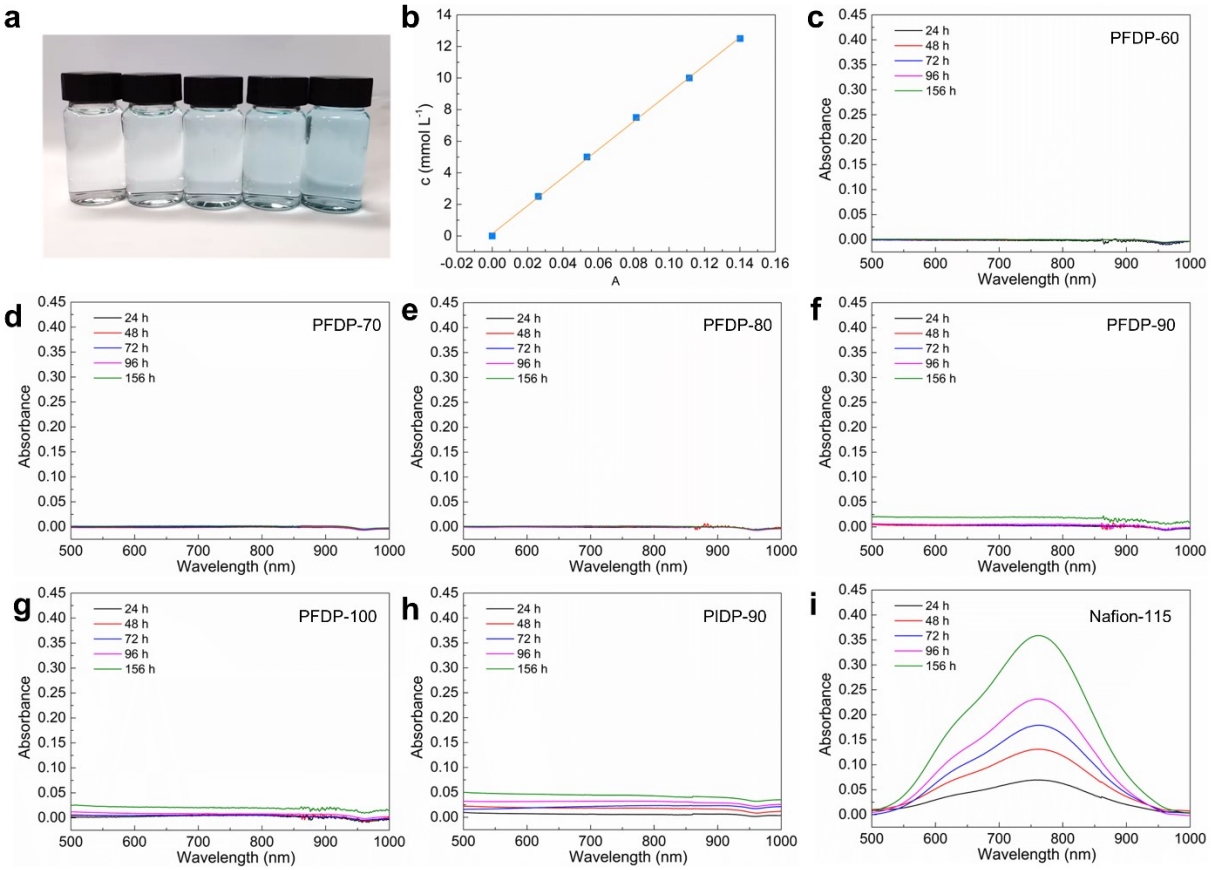

Fig. S16 a) Equal gradient dilutions of standard VO^{2+} ion solutions in 50 mL volumetric flasks. b) The standard curve for VO^{2+} solution. Percolation diffusion test of $VOSO_4$ through different ionic membranes. The UV-Vis spectra of $VOSO_4$ on the permeate side were investigated with c) PFDP-60; d) PFDP-70; e) PFDP-80; f) PFDP-90; g) PFDP-100; h) PIDP-90 and i) Nafion 115 membrane assembly tests over time.

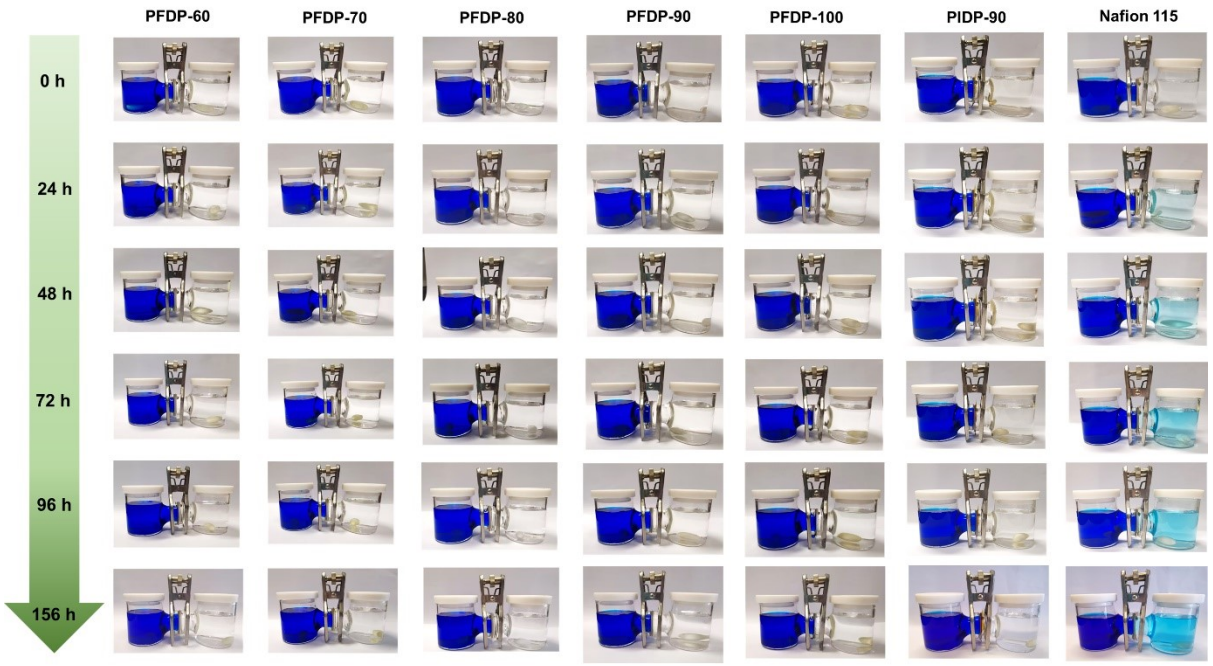

Fig S17 Photographs showing the color change at the beginning (0 h) to the end (156 h) of the permeate solution are displayed in the figure, and samples are taken at certain intervals for testing and photographic documentation. The electrolyte is 3 M H_2SO_4 aqueous solution on the feed and permeate side. The $MgSO_4$ solution that remains colorless on the permeate side indicates that VO^{2+} permeates at a slower rate in the PFDP-x membrane, whereas in the same Nafion 115 H cell a significant color change is observed on the permeate side even within 24 h. Thus, VO^{2+} permeates at least one order of magnitude faster in the Nafion 115 membrane.

Table S3. Comparison of swelling ratio, area resistance and vanadium permeability of AEMs with different molecular designs and Nafion membranes.

Membranes	Swelling ratio (%)	Area resistance (Ω cm^2)	Vanadium permeability (cm^2 min^{-1})	Ref.
PFDP-60	1.59	0.78	1.32×10^{-9}	This work
PFDP-70	2.86	0.40	1.95×10^{-9}	This work
PFDP-80	4.30	0.25	2.88×10^{-9}	This work
PFDP-90	5.85	0.19	1.02×10^{-8}	This work
PFDP-100	7.66	0.17	1.44×10^{-8}	This work
PyPEKK30	1.80	0.40	3.4×10^{-7}	[1]
PyPEKK50	7.10	0.28	6.8×10^{-7}	[1]
PyPEKK90	28.60	0.15	1.74×10^{-6}	[1]
p-TPN1	-	0.29	0.74×10^{-7}	[2]
m-TPN1	-	0.27	1.26×10^{-7}	[2]
BPN1-100	-	0.22	2.38×10^{-6}	[2]
FAP-450	-	0.72	7.09×10^{-7}	[2]
Nafion 212	-	0.23	4.12×10^{-6}	[2]
Nafion 117	-	0.89	3.21×10^{-6}	[2]
PTMIm	-	0.61	1.1×10^{-7}	[3]
PTMIm-C3-QA	-	0.75	9.5×10^{-9}	[3]
PBI	>10	0.78	2.0×10^{-7}	[4]
PBI-9%EPTMA	>13	0.62	1.0×10^{-7}	[4]
PBI-21%EPTMA	>40	0.41	5.1×10^{-7}	[4]
PBI-42%EPTMA	>50	0.31	9.9×10^{-7}	[4]
PSf-Im-1.2	9.1	0.90	8.52×10^{-7}	[5]
PSf-Mim-1.2	19.8	0.80	18.12×10^{-7}	[5]
PSf-PhIm-1.2	8.5	1.40	7.50×10^{-7}	[5]
PSf-PhBIm-1.2	6.3	1.80	0.50×10^{-7}	[5]
Nafion 115	3.9	1.00	12.95×10^{-7}	[5]

Note: Swelling ratio and area resistance were measured at RT in 3.0 M H_2SO_4 solution. The permeation test cell was filled with 1.5 M $VOSO_4$ in 3.0 M H_2SO_4 solution and 1.5 M $MgSO_4$ in 3.0 M H_2SO_4 solution, respectively.

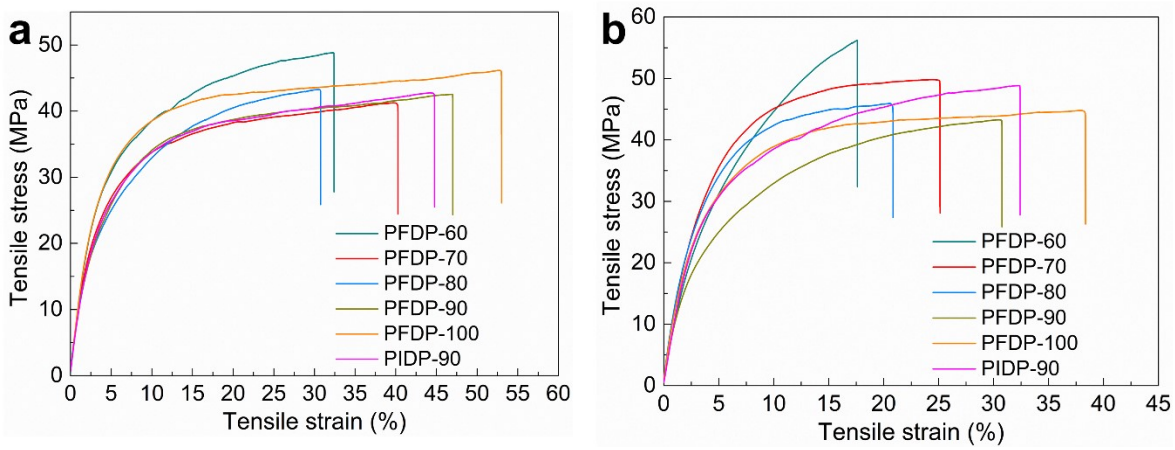

Fig. S18 Stress-strain curves of PFDP and PIDP AEMs. a) mechanical properties of the membrane after absorbing water, b) mechanical properties of the membrane after absorbing acid.

Table S4. Tensile strength (TS), elongation at break (EB) and Young's modulus (YM) of AEMs at room temperature

AEMs	TS[a]	EB[a]	YM[a]	TS[b]	EB[b]	YM[b]	TS[c]	EB[c]	YM[c]	Ref.
PFDP-60	61.99	18.63	1.75	48.84	32.4	1.06	56.18	17.6	0.96	This work
PFDP-70	62.68	11.14	1.84	41.26	40.27	1.03	49.82	25.13	1.23	This work
PFDP-80	47.21	13.78	1.37	43.23	30.75	0.98	45.94	20.83	1.31	This work
PFDP-90	45.16	15.39	1.03	42.55	46.99	0.94	43.27	30.75	0.98	This work
PFDP-100	49.81	25.13	1.23	46.15	53.01	1.05	44.79	38.36	1.22	This work
PIDP-90	49.28	12.12	0.93	42.77	44.76	0.93	48.84	32.4	1.05	This work
PTP-TFA	-	-	-	-	-	-	36.4	7.2	-	[6]
PTP-Me	-	-	-	-	-	-	33.5	10.3	-	[6]
PTP-CHPTMA	-	-	-	-	-	-	32.7	14.6	-	[6]
PTMIm	-	-	-	-	-	-	35.2	17.2	-	[3]
PTMIm-C3	-	-	-	-	-	-	33.1	17.4	-	[3]
PTMIm-C3 -QA	-	-	-	-	-	-	31.7	11.3	-	[3]
PTMIm-C3-OH-QA	-	-	-	-	-	-	23.4	11.2	-	[3]
PSf-Im 1.2	-	-	-	17.3	18.3	-	-	-	-	[5]
PSf-MIm 1.2	-	-	-	10.8	36.4	-	-	-	-	[5]
PSf-PhIm 1.2	-	-	-	20.6	17.5	-	-	-	-	[5]
PSf-PhBIm 1.2	-	-	-	3.3	11.0	-	-	-	-	[5]

[a] Mechanical properties of the membrane in the dry state.

[b] Mechanical properties of the membrane after absorbing water.

[c] Mechanical properties of the membrane after absorbing acid.

-: Not mentioned.

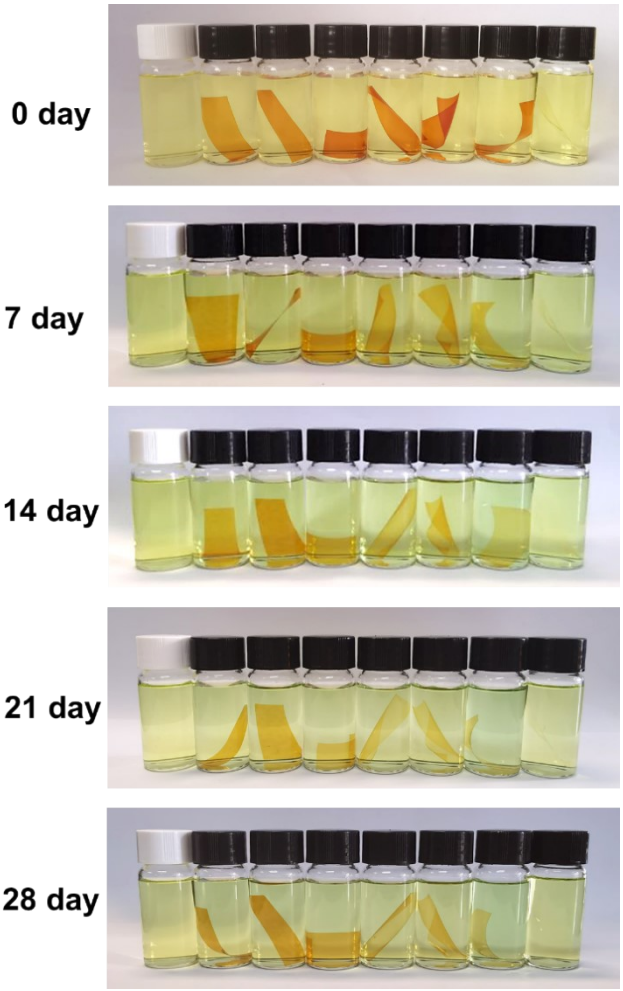

Fig. S19 Digital photographs of seven ion exchange membranes immersed in 0.1 M VO_2^+ + 3 M H_2SO_4 solution with time (from left to right, blanks, PFDP-60, PFDP-70, PFDP-80, PFDP-90, PFDP-100, PFDP-90, Nafion 115 membranes).

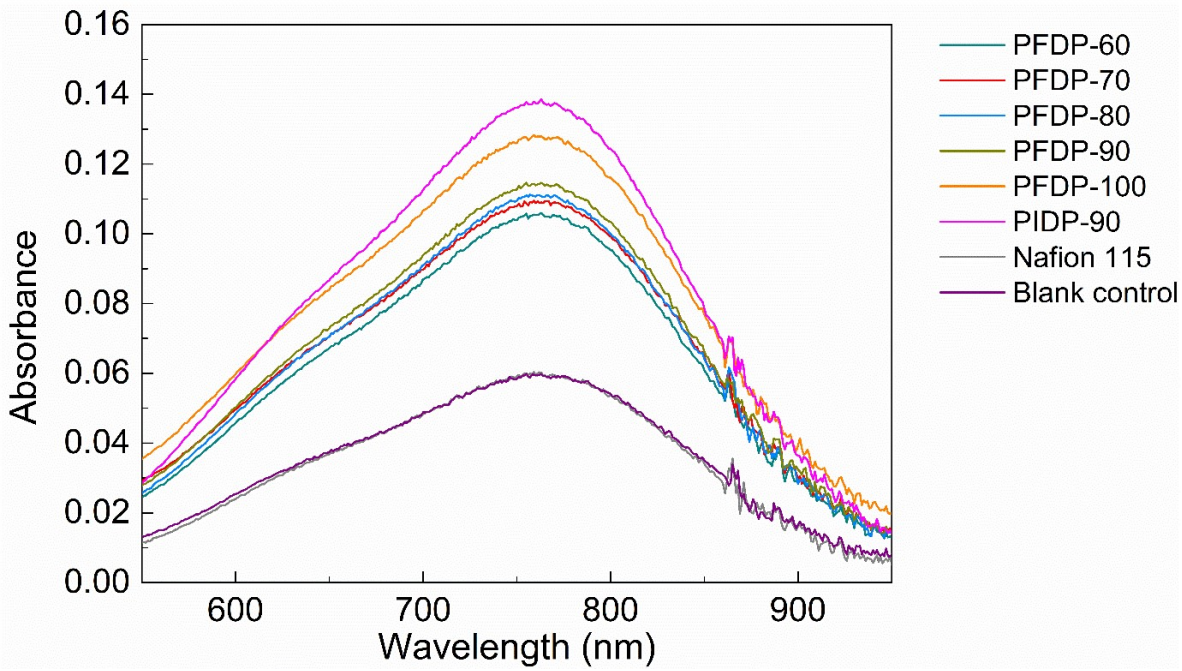

Fig. S20 PFDP-x, PIDP-90 and Nafion 115 membranes were immersed in 0.1 M VO_2^+ + 3 M H_2SO_4 solution for 28 days, and the UV-Vis spectrum (VO^{2+}) of the immersion solution was measured.

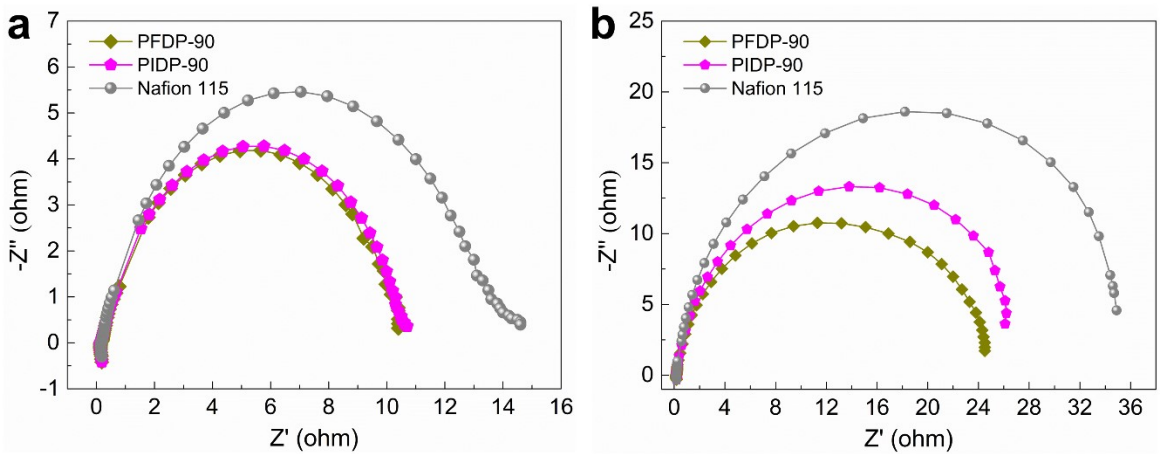

Fig. S21 EIS curves of VFB single cells assembled with PFDP-90, PIDP-90 and Nafion 115 membrane under different conditions: (a) Nyquist plot after the electrolyte was introduced into the cell and stand for 30 minutes; (b) Nyquist plot after 50 cycles at 120 mA cm^{-2}.

Table S5. Comparison of recently reported unmodified polymeric ion exchange membranes for VFB single cells.

Sample	Current density (mA cm^{-2})	EE（%）	Ref.
PFDP-90	60	86.75	This work
	120	83.14	
QPPP-2	100	~82	[7]
	120	~80	
p-TPN1	100	~84	[2]
PBI-21%EPTMA	100	~81	[4]
PAES-8mPip-25	40	86.5	[8]
	60	85.44	
	80	84.3	
DQA-TAPFE-20	40	~83	[9]
	60	~81	
	80	~79	
PTMIm-C3-QA	80	~80	[3]
	120	~72	
TM-OPBI-12	100	~80	[10]
	120	~76	
HSPAEK	40	90.2	[11]
	120	76	
6F-SPI-50	20	~85	[12]
	60	~74	
6F-s-bSPI	40	~83	[13]
	80	~73	
sPBPSP-8	100	~80	[14]
	120	~77	
SPI50	100	82.5	[15]
	120	~80	
S-L-PPO-51%	100	83.43	[16]
	120	81.85	
S/SMA-SN-0.5	100	~81	[17]
	120	~80	

References

[1] B.G. Zhang, M.H. Zhao, Q. Liu, X.T. Zhang, Y.S. Fu, E.L. Zhang, G.S. Wang, Z.G. Zhang, X.C. Yuan, S.H. Zhang, High performance membranes based on pyridine containing poly (aryl ether ketone ketone) for vanadium redox flow battery applications, J. Power Sources 506 (2021) 230128. https://doi.org/10.1016/j.jpowsour.2021.230128.

[2] T.S. Wang, J.Y. Jeon, J. Han, J.H. Kim, C. Bae, S. Kim, Poly(terphenylene) anion exchange membranes with high conductivity and low vanadium permeability for vanadium redox flow batteries (VRFBs), J. Membr. Sci. 598 (2020) 117665.

[3] T. Mu, W.Q. Tang, N. Shi, G.R. Wang, T.T. Wang, T. Wang, J.S. Yang, Novel ether-free membranes based on poly(p-terphenylene methylimidazole) for vanadium redox flow battery applications, J. Membr. Sci. 659 (2022) 120793.

[4] X.R. Ren, L.N. Zhao, X.F. Che, Y.Y. Cai, Y.Q. Li, H.H. Li, H. Chen, H.X. He, J.G. Liu, J.S. Yang, Quaternary ammonium groups grafted polybenzimidazole membranes for vanadium redox flow battery applications, J. Power Sources 457 (2020) 228037.

[5] Y. Xing, K. Geng, X.M. Chu, C.Y. Wang, L. Liu, N.W. Li, Chemically stable anion exchange membranes based on C2-Protected imidazolium cations for vanadium flow battery, J. Membr. Sci. 618 (2021) 118696.

[6] W.Q. Tang, T. Mu, X.F. Che, J.H. Dong, J.S. Yang, Highly selective anion exchange membrane based on quaternized poly(triphenyl piperidine) for the vanadium redox flow battery, ACS Sustain. Chem. Eng. 9 (2021) 14297-14306.

[7] M.S. Cha, S.W. Jo, S.H. Han, S.H. Hong, S. So, T.H. Kim, S.G. Oh, Y.T. Hong, J.Y. Lee, Ether-free polymeric anion exchange materials with extremely low vanadium ion permeability and outstanding cell performance for vanadium redox flow battery (VRFB) application, J. Power Sources 413 (2019) 158-166.

[8] Z.W. Tao, C.Y. Wang, S.J. Cai, J.F. Qian, J. Li, Efficiency and oxidation performance of densely flexible side-chain piperidinium-functionalized anion exchange membranes for vanadium redox flow batteries, ACS Appl. Energy Mater. 4 (2021) 14488-14496.

[9] Y. Chen, Y.Y. Li, J.Q. Xu, S.Y. Chen, D.Y. Chen, Densely quaternized fluorinated poly(fluorenyl ether)s with excellent conductivity and stability for vanadium redox flow

batteries, ACS Appl. Mater. Interfaces 13 (2021) 18923-18933.

[10] L.M. Ding, L.H. Wang, Preparation of novel structure polybenzimidazole with thiophene ring for high performance proton conducting membrane in vanadium flow battery, J. Power Sources 564 (2023) 232858.

[11] B.B. Yin, Z.H. Li, W.J. Dai, L. Wang, L.H. Yu, J.Y. Xi, Highly branched sulfonated poly(fluorenyl ether ketone sulfone)s membrane for energy efficient vanadium redox flow battery, J. Power Sources 285 (2015) 109-118.

[12] J.C. Li, S.Q. Liu, Z. He, Z. Zhou, Semi-fluorinated sulfonated polyimide membranes with enhanced proton selectivity and stability for vanadium redox flow batteries, Electrochim Acta 216 (2016) 320-331.

[13] J.C. Li, S.Q. Liu, Z. He, Z. Zhou, A novel branched side-chain-type sulfonated polyimide membrane with flexible sulfoalkyl pendants and trifluoromethyl groups for vanadium redox flow batteries, J. Power Sources 347 (2017) 114-126.

[14] H.Y. Shin, M.S. Cha, S.H. Hong, T.H. Kim, D.S. Yang, S.G. Oh, J.Y. Lee, Y.T. Hong, Poly(p-phenylene)-based membrane materials with excellent cell efficiencies and durability for use in vanadium redox flow batteries, J. Mater. Chem. A 5 (2017) 12285-12296.

[15] L. Wang, L.H. Yu, D. Mu, L.W. Yu, L. Wang, J.Y. Xi, Acid-base membranes of imidazole-based sulfonated polyimides for vanadium flow batteries, J. Membr. Sci. 552 (2018) 167-176.

[16] X.M. Yan, J.H. Sun, L. Gao, W.J. Zheng, Y. Dai, X.H. Ruan, G.H. He, A novel long-side-chain sulfonated poly(2,6-dimethyl-1,4-phenylene oxide) membrane for vanadium redox flow battery, Int. J. Hydrog. Energy 43 (2018) 301-310.

[17] S. Jiang, H.X. Wang, L. Li, C.Y. Zhao, J.X. Sheng, H.F. Shi, Improvement of proton conductivity and efficiency of SPEEK-based composite membrane influenced by dual-sulfonated flexible comb-like polymers for vanadium flow battery, J. Membr. Sci. 671 (2023) 121394.